

## Energy-efficient sorption-based gas clothes dryer systems

Masoud Ahmadi<sup>a</sup>, Kyle R. Gluesenkamp<sup>b</sup>, Sajjad Bigham<sup>a,\*</sup>

<sup>a</sup> Department of Mechanical Engineering-Engineering Mechanics, Michigan Technological University, 1400 Townsend Drive, Houghton, MI 49931-1295, USA

<sup>b</sup> Building Technologies Research and Integration Center, Oak Ridge National Laboratory, One Bethel Valley Road, P.O. Box 2008, MS-6070, Oak Ridge, TN 37831-6070, USA

### ARTICLE INFO

#### Keywords:

Dehydration  
Sorption-based systems  
Gas-driven systems  
Advanced gas clothes dryer systems  
Dehumidification  
Moisture latent heat

### ABSTRACT

Standard electric resistance and fuel-driven dehydration technologies exhibit a maximum coefficient of performance of well below 1 mainly due to enthalpy losses associated with the air leaving the dehydration system. To improve energy efficiency, condensing dryer systems condense the moisture captured from a product in a closed-loop air circulation cycle. Existing condensing dehydration systems including heat pump dryers, however, need to significantly cool the air to achieve dehumidification. The added cooling and subsequent heating to return the air to a desired drying temperature consume substantial energy and thus reduce drying performance. Here, an innovative sorption-based gas dehydration system is proposed to overcome barriers deteriorating energy efficiency in existing gas, electric, or heat pump dryer systems. Decoupling latent and sensible loads, the system employs a liquid-desiccant solution to directly capture air humidity, thereby allowing circulation of the air in a closed loop to achieve high drying energy efficiency. In other words, the system captures waste latent heat from the moisture produced during the dehydration process and reuses it to improve energy efficiency. This study focuses on a comprehensive quasi-steady-state thermodynamic modeling of the proposed sorption-based dehydration concept employed for a gas clothes dryer application to predict transient response and overall drying performance (i.e., time and energy metrics). The analysis indicates the proposed sorption-based gas clothes dryer system can deliver a specific moisture extraction rate of 1.71 kg of water per kWh (i.e., a combined energy factor of 3.167 kg (6.98 lbm) of dry cloth per kWh) with a drying time of 44 min. This is a 112% energy improvement compared with state-of-the-art gas clothes dryers exhibiting a combined energy factor of 1.50 kg (3.3 lbm) of dry cloth per kWh. The technology pursued here can potentially be employed as a platform for many fuel-driven equipment to take advantage of available waste thermal energy in the environment instead of simply burning a fuel.

### 1. Introduction

Dehydration is a ubiquitous process often representing one of the most energy-intensive steps in various industrial, residential, and commercial applications, reflecting up to 15% of the overall world industrial energy consumption [1,2]. In the residential sector, clothes dryer systems have become one of the major building appliances, reflecting 6% of the total US residential electricity consumption [3–8]. A large fraction of this energy usage is attributed to a high moisture content produced during the drying of wet products. Latent heat associated with product moisture, however, can be viewed as a potential new energy source offering a unique way to reduce the energy consumption of various drying applications.

In conventional dehydration systems, ambient air heated by an

electric resistance or more commonly a fossil fuel (e.g., petroleum, coal, or natural gas) source with a maximum theoretical coefficient of performance (COP) of 1 drives the drying process. Once saturated with moisture, the air leaves the dryer system at a temperature between that of the ambient and the dryer inlet. Although it is a low capital cost solution for many residential, commercial, and industrial applications, this class of dehydration systems suffers from a low energy efficiency, mainly due to enthalpy losses associated with the vented warm air.

The simplest strategy to improve the drying energy efficiency is to recuperate a portion of waste heat associated with the vented air. Bansal et al. [9] compared conventional and heat-recovery clothes dryer systems under different working conditions. They determined that drying energy efficiency and specific moisture extraction rate defined as energy input per unit load highly depend on the effectiveness of the recovery

\* Corresponding author.

E-mail addresses: [sbigham@mtu.edu](mailto:sbigham@mtu.edu), [bighams@ufl.edu](mailto:bighams@ufl.edu) (S. Bigham).

<https://doi.org/10.1016/j.enconman.2020.113763>

Received 9 October 2020; Accepted 10 December 2020

Available online 3 January 2021

0196-8904/© 2020 Elsevier Ltd. All rights reserved.

heat exchangers utilized. Jian and Luo [10] utilized a heat pipe recovery exchanger to improve the energy performance of a venting tumble clothes dryer. They realized a 17.6% reduction in electricity consumption compared with a standard clothes dryer without a heat recovery unit.

To further improve drying energy efficiency, condensing dehydration systems condense the moisture in a closed-loop air circulation cycle. This is achieved either by a simple air/water-cooled condensing heat exchanger [11,12] or more commonly a heat pump dryer (HPD). A HPD system could utilize either a vapor compression refrigeration (VCR) cycle [5,9,13–19] or an absorption refrigeration cycle [20–25]. Here, the product moisture is condensed in the evaporator module of the heat pump cycle. The dehumidified air is then heated in the condenser module of the VCR unit or both absorber and condenser modules in the case of absorption-driven HPD before sending back to the dryer section. Cochran et al. [11] studied the performance of an air-cooled condensing dryer utilizing a surface tension element as the condensing heat exchanger. The surface tension element improved the drying energy efficiency by 4% at a reduced operating temperature and drying time. Utilizing a VCR-based heat pump dryer, TeGrotenhuis et al. [6] reported energy savings of as high as 50% compared with standard residential clothes dryers. Cao et al. [19] proposed a two-stage VCR-based heat pump clothes dryer and achieved 59% energy savings and 143% improvement in energy factor (EF) in comparison with conventional electric dryers. Additionally, drying of food, lignite, and wood products were reported to be faster and economically favorable through VCR-based heat pump drying systems [1,26–31]. Furthermore, prior studies have shown that absorption-based heat pump drying system could reduce drying energy efficiency by up to 20% for various industrial applications [20–25]. Existing condensing dehydration systems, however, need to significantly cool the air to achieve the dehumidification process. The added cooling and subsequent heating to return the air to a desired drum temperature consume substantial energy and thus reduce drying energy efficiency.

Eliminating usage of refrigerants with a high global warming potential (GWP), solid-state thermoelectric (TE) heat pump dryers [4,32] offer an alternative approach to improve drying performance. Experiments conducted by Patel et al. [4] demonstrated an energy factor as high as 6.51 lbm of dry cloth per kWh of electric energy consumed with a dry time of 159 min. Current issues associated with TE-based dryers are long drying cycle times and added system complexity.

The above literature review clearly indicates that existing drying systems cannot effectively leverage high temperatures associated with the vented dryer air. Here, a novel fuel-driven dehydration concept is introduced to overcome shortcomings inherent to current drying technologies. Decoupling latent and sensible loads, the new drying concept enables to simultaneously dehumidify and heat the vented air at elevated temperatures rather than cooling the vented air for the dehumidification process. This functionality, currently unavailable in existing dehydration systems, significantly improves drying performance metrics. The proposed system consumes natural gas to drive a desiccant-based thermodynamic cycle to effectively use latent heat associated with the product moisture as an advantageous energy source. Compared with VCR-based heat pump dryers, the proposed system eliminates the usage of high GWP refrigerants. In the following sections, first, the proposed drying concept is discussed. A quasi-steady-state thermodynamic model is then developed to evaluate transient response and overall performance of the system. Finally, transient behavior and overall drying performance of the proposed sorption-based gas dehydration concept employed for a gas clothes dryer application are discussed for different hydro-thermodynamic conditions.

## 2. Concept

The proposed sorption-based gas dehydration concept employs a novel drying approach effectively capturing the waste latent heat from

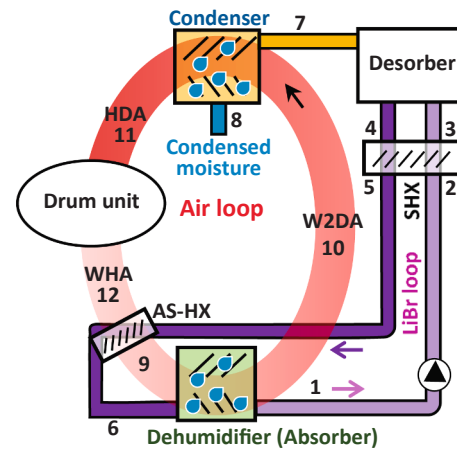


Fig. 1. A schematic of the proposed sorption-based gas dehydration concept. WHA, W2DA, and HDA are warm humid air, warmer dry air, and hot dry air, respectively.

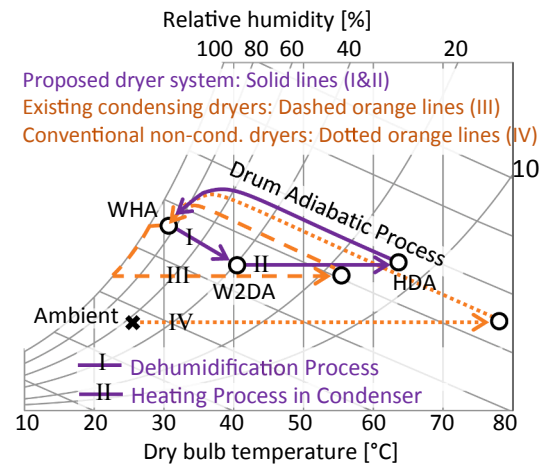


Fig. 2. Representative psychrometric air flow processes of various dehydration systems.

the warm humid air (WHA) leaving the drum unit, and reusing it to improve the system's energy efficiency. Fig. 1 shows the components and operating principles of the proposed dryer concept. At the heart of the system, there is a membrane-based lithium bromide (LiBr) dehumidifier module [33–35] that directly absorbs the humidity of the WHA leaving the dryer. The direct absorption process indeed enables circulation of the dehumidified air at high temperatures, thereby leveraging the enthalpy of dryer outlet warm air. This process contrasts the proposed technology with standard drying systems that vent (in conventional dryers) or cool (in condensing dryers) the air, either of which spoils the available enthalpy of the dryer outlet warm air. The heat released during the absorption process is partially transferred to the air flow stream, raising its temperature to a warmer dry air (W2DA) state (cf., Fig. 1). As shown in the LiBr loop, the absorbed humidity is thermally rejected from the LiBr solution in the desorber module and subsequently condensed in a condenser heat exchanger. The heat of the condensation process is also transferred to the air flow stream, further increasing its temperature to a hot dry air (HDA) state before flowing back to the dryer. In other words, the proposed sorption-based gas dehydration system effectively utilizes the latent heat associated with the moisture twice: once during the dehumidification and again during the subsequent condensation process. This substantially improves the

overall system energy efficiency. The desorption process is driven by heat generated by a natural gas burner.

Fig. 2 illustrates the air flow psychrometric processes of various dehydration technologies. As shown, the latent heat released during the moisture absorption process (i.e., process I) increases air temperature from the WHA to W2DA state. The temperature of the dehumidified air is then further increased from the W2DA to HDA state by the latent heat released in the condenser module of the liquid-desiccant system (process II). It should be noted that the same product moisture deteriorates the dehydration performance in state-of-the-art condensing dryer systems as can be perceived by the dashed lines in process III. The air processes of the non-condensing dryers (i.e., the dotted lines in process IV) are also shown for reference.

### 3. Modeling

The present study focuses on a comprehensive quasi-steady-state thermodynamic cycle modeling of the proposed sorption-based gas dehydration concept employed for a clothes dryer system. The thermodynamic model predicts transient response and overall drying performance of the proposed system. The thermodynamic model developed in Engineering Equation Solver (EES) includes the entire system shown in Fig. 1. The transient behavior of the desiccant loop was mathematically modeled based on the authors' prior publications on absorption systems [33–35]. The transient nature of the dryer module is modeled using the mass and energy balance equations. Solving the two interactive sorption and dehydration sub-models results in the calculation of important features of the proposed dehydration concept, including the specific moisture extraction rate (SMER), combined energy factor (CEF), and total drying time. Equations solved in each sub-model and the algorithm utilized are explained in more detail in the following sections.

#### 3.1. Sorption sub-model

The sorption sub-model considers the mass and energy balance equations of each individual module shown in Fig. 1. The sorption loop performs both dehumidification and heating of the recirculated air. The strong LiBr solution entering the absorber module first captures the air humidity. The heat released during the absorption process increases both air and solution temperatures. The weak solution leaving the absorber module is then pumped to the desorber module. In the desorber unit, the captured water vapor is endothermically desorbed from the LiBr solution and subsequently condensed in the condenser module. The condenser is an indirect heat exchanger in which the latent heat of the condensation process is transferred to the air stream. The strong LiBr solution leaving the desorber then flows back to the dehumidifier module to complete the LiBr cycle.

##### 3.1.1. Dehumidifier module

The dehumidification process is enabled by a difference in the water vapor pressure between the air and solution sides. The mass and energy balance equations listed below mathematically describe the dehumidifier (absorber) module.

$$\dot{m}_{1,solution} = \dot{m}_{6,solution} + \dot{m}_{7,vapor} \quad (1)$$

$$\dot{m}_{1,solution}x_1 = \dot{m}_{6,solution}x_6 \quad (2)$$

$$\dot{Q}_{dehum} = \dot{m}_{6,solution}h_6 + \dot{m}_{7,vapor}h_{7,vapor} - \dot{m}_{1,solution}h_1 \quad (3)$$

where  $\dot{m}$ ,  $x$ ,  $h$ , and  $\dot{Q}_{dehum}$  are mass flow rate, LiBr concentration, enthalpy, and heat transfer rate of the dehumidifier module, respectively. Additionally, the energy exchanged between the air and solution streams can be calculated by the logarithmic mean temperature difference (LMTD) [36] as follows:

$$\dot{m}_{dry-air}(h_{10} - h_9) = (UA)_{dehum}LMTD_{dehum} \quad (4)$$

$$LMTD_{dehum} = \frac{(T_1 - T_6) - (T_9 - T_{10})}{\ln\left(\frac{T_1 - T_6}{T_9 - T_{10}}\right)} \quad (5)$$

where  $U$ ,  $A$ , and  $T$  are overall heat transfer coefficient, overall surface area, and temperature, respectively.

##### 3.1.2. Desorber module

The absorbed humidity is thermally rejected from the LiBr solution in the desorber module. The thermal energy required for the desorption process can be calculated by applying the mass and energy balance equations as follows:

$$\dot{m}_{3,solution} = \dot{m}_{4,solution} + \dot{m}_{7,vapor} \quad (6)$$

$$\dot{m}_{3,solution}x_3 = \dot{m}_{4,solution}x_4 \quad (7)$$

$$\dot{Q}_{des} = \dot{m}_{4,solution}h_4 + \dot{m}_{7,vapor}h_7 - \dot{m}_{3,solution}h_3 \quad (8)$$

where  $\dot{Q}_{des}$  is the thermal energy supplied to the desorber module of the system. The thermal energy can also be written as the overall heat transfer coefficient as

$$\dot{Q}_{des} = (UA)_{des}LMTD_{des} \quad (9)$$

$$LMTD_{des} = \frac{(T_{hot\_oil\_in} - T_4) - (T_{hot\_oil\_out} - T_7)}{\ln\left(\frac{T_{hot\_oil\_in} - T_4}{T_{hot\_oil\_out} - T_7}\right)} \quad (10)$$

where  $T_{hot\_oil\_in}$  and  $T_{hot\_oil\_out}$  are temperatures of a hot oil stream entering and leaving the desorber module, respectively.

##### 3.1.3. Condenser module

The desorbed vapor is condensed in the condenser module. The latent heat of the condensation process is then transferred to the air flow stream. The condenser module is an indirect heat exchanger unit as described by the following energy balance equations:

$$\dot{Q}_{cond} = \dot{m}_{vapor}(h_7 - h_8) = (UA)_{cond}LMTD_{cond} \quad (11)$$

$$LMTD_{cond} = \frac{(T_7 - T_8) - (T_{10} - T_{11})}{\ln\left(\frac{T_7 - T_8}{T_{10} - T_{11}}\right)} \quad (12)$$

where  $\dot{Q}_{cond}$  is the heat transfer rate of the condenser module.

##### 3.1.4. Solution heat exchanger (SHX)

The solution heat exchanger transfers heat from the hot strong solution to the cold weak solution, thereby improving the efficiency of the system. The overall energy balance for the solution heat exchanger can be written as

$$\dot{m}_{4,solution}h_4 - \dot{m}_{5,solution}h_5 = \dot{m}_{3,solution}h_3 - \dot{m}_{2,solution}h_2 \quad (13)$$

The effectiveness of the solution heat exchanger unit ( $\epsilon_{SHX}$ ) can also be described as

$$\epsilon_{SHX} = \frac{T_4 - T_5}{T_4 - T_2} \quad (14)$$

##### 3.1.5. Solution pump

A solution pump is used to circulate the desiccant solution. Considering an isentropic process and incompressible flow, the enthalpy rise across the solution pump can be calculated as

$$h_2 = h_1 + \nu_1(P_h - P_l) \quad (15)$$

where  $P_h - P_l$  and  $\nu$  are the pressure difference between the desorber and absorber modules in an open desiccant cycle and specific volume, respectively. The pump work is then calculated as

$$\dot{W}_{pump} = \dot{m}_{1,solution}(h_2 - h_1) \quad (16)$$

### 3.1.6. Air-to-solution heat exchanger (AS-HX)

The temperature of the air leaving the dryer module tends to increase when the remaining moisture content (RMC) of the product decreases. This is attributed to the heat and mass transfer effectiveness of the dryer module, which deteriorates at the later stages of the drying process. This, in turn, increases the overall operating temperature of the sorption cycle and thus reduces the dehumidification rate. Therefore, an air-to-solution heat exchanger is utilized to further decrease the temperature of the strong solution before entering the absorber module. The energy balance equations for the AS-HX unit can be expressed as

$$\dot{Q}_{AS-HX} = \dot{m}_{air}(h_9 - h_{12}) = \dot{m}_{solution}(h_5 - h_6) = (UA)_{AS-HX} LMTD_{AS-HX} \quad (17)$$

$$LMTD_{AS-HX} = \frac{(T_5 - T_6) - (T_9 - T_{12})}{\ln\left(\frac{T_5 - T_6}{T_9 - T_{12}}\right)} \quad (18)$$

### 3.2. Dehydration sub-model

The efficiency of the drying process depends on several factors, including the shape of a product (i.e., form factor), the geometry of the drum unit, and flow distributions. These factors affect the heat and mass transfer processes involved and can be summarized as the heat and mass transfer effectiveness. The heat transfer effectiveness is defined as the ratio of actual heat transfer ( $Q$ ) to the maximum possible heat transfer ( $Q_{max}$ ) between the air and the cloth being dehydrated:

$$\varepsilon_H = \frac{Q}{Q_{max}} = \frac{T_{12} - T_{11}}{T_{surf} - T_{11}} \quad (19)$$

Similarly, the mass transfer effectiveness is defined as the ratio of actual mass transfer ( $J$ ) to maximum possible mass transfer ( $J_{max}$ ) between the air stream and the cloth moisture content:

$$\varepsilon_M = \frac{J}{J_{max}} = \frac{\omega_{12} - \omega_{11}}{\omega_{surf} - \omega_{11}} \quad (20)$$

where  $\omega$  is air humidity ratio. Here, the heat and mass transfer effectivenesses are assumed to be equal (i.e.,  $\varepsilon_H = \varepsilon_M$ ). Additionally, the moisture present at the surface of the product is assumed to be at a saturated condition as

$$\omega_{surf} = \omega_{sat} = \frac{0.622P_{w,sat}|_{T_{surf}}}{P_{atm} - P_{w,sat}|_{T_{surf}}} \quad (21)$$

Additionally, the drying process is a transient mass transfer event affecting the mass of water present in the product as follows:

$$m_{water,i+1} = m_{water,i} - \dot{m}_{air}(\omega_{12} - \omega_{11}) \quad (22)$$

where subscripts  $i$  and  $i + 1$  stand for mass of water present in the product at two subsequent drying time steps. The transient remaining moisture content ( $RMC_i$ ) can be then defined as the ratio of the transient mass of water trapped inside the fabric to the bone-dry product as follows:

$$RMC_i = \frac{m_{water,i}}{m_{bonedrycloth}} \quad (23)$$

Considering the unsteady heat transfer nature of the dehydration process, the drum unit energy balance equation can be expressed as

$$\dot{Q}_{air}\Delta t = Q_{dryerframe} + Q_{bonedrycloth} + Q_{water} + \dot{Q}_{loss}\Delta t \quad (24)$$

where  $\Delta t$  is the time difference between two subsequent drying time steps  $i$  and  $i + 1$ . Here, the total energy exchanged with the air stream is divided into four separate loads: sensible heat associated with the solid materials such as the drum, baffles, ducts, vents, and frame collectively referred to as  $Q_{dryerframe}$ , sensible heat interacted with the cloth ( $Q_{bonedrycloth}$ ), sensible and latent thermal energy interacted with water ( $Q_{water}$ ), and dryer heat loss rate ( $\dot{Q}_{loss}$ ). The temperature distribution throughout the metal frame, cloth, and water is considered uniform and equal to cloth surface temperature ( $T_{surf}$ ) (i.e., a lumped system analysis). Additionally, the drum heat loss rate is assumed to be 15% of the air heat transfer rate. The total energy exchanged with the air stream, thermal energy of the dryer frame, internal energy associated with the cloth, and thermal energy exchanged with water are defined as

$$\dot{Q}_{air} = \dot{m}_{air}(h_{11} - h_{12}) \quad (25)$$

$$Q_{dryer\ frame} = m_{frame}c_{p,frame}(T_{surf,i+1} - T_{surf,i}) \quad (26)$$

$$Q_{bone\ dry\ cloth} = m_{bone\ dry\ cloth}c_{p,cloth}(T_{surf,i+1} - T_{surf,i}) \quad (27)$$

$$Q_{water} = (m_{water,i+1}T_{surf,i+1} - m_{water,i}T_{surf,i})c_{p,water} + (m_{water,i+1} - m_{water,i})h_{fg} \quad (28)$$

$$\dot{Q}_{loss} = 0.15\dot{Q}_{air} \quad (29)$$

where  $c_p$  and  $h_{fg}$  are specific heat capacity and latent heat of vaporization of water, respectively.

### 3.3. Overall performance characteristics

The present study focuses on evaluating the proposed sorption-based gas dehydration concept for a clothes dryer application. Metrics considered to characterize the overall performance of the system are SMER, CEF, and drying time. The US Department Of Energy (DOE) Code of Federal Regulations "10 CFR Part 430," Subpart B, Appendix D1, "Uniform Test Method for Measuring the Energy Consumption of Clothes Dryers" was employed as the test procedure [37]. The CEF and drying time are calculated to dry 3.83 kg (8.45 lbm) of cloth from an initial RMC of 57.5% to 4% [38] per equivalent kWh of energy consumed. The electrical power required to rotate the drum is assumed to be equal to 150 W. Electrical power for the air blower motor is considered as a function of air flow rate as follows [4]:

$$\dot{W}_{blower} = C_{cl}\left(0.0107\dot{Q}^2 - 0.7845\dot{Q} + 25.194\right)[W], \quad C_{cl} = 1.19 \quad (30)$$

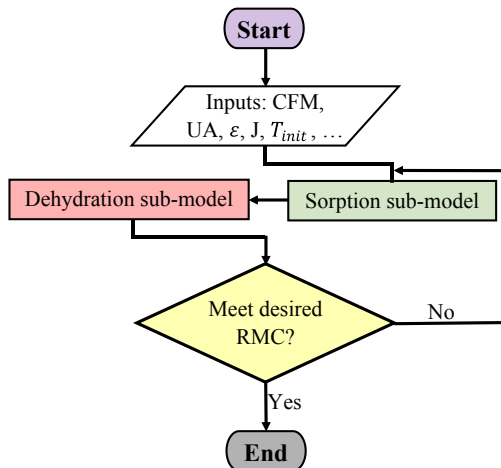


Fig. 3. Modeling flowchart.

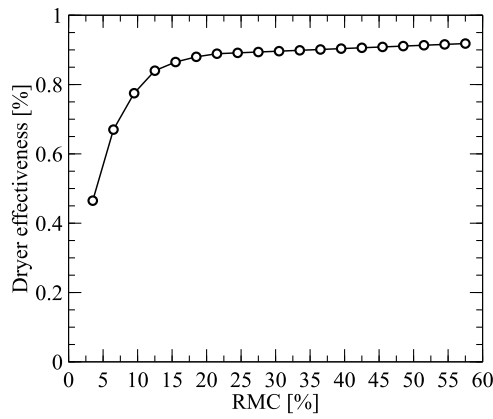


Fig. 4. Heat and mass transfer effectiveness of a sample clothes dryer at different RMCs [39].

Table 1  
Nominal and constant input parameters to the thermodynamic model.

| Parameter   | Value [unit]               |
|---|----------------------------|
| Bone-dry cloth mass   | 3.83 [kg]                  |
| Heat capacity of cloth (i.e., cotton)   | 1.4 [kJ/kg-K]              |
| Effective mass of the clothes dryer frame (i.e., stainless steel) including drum, baffles, ducts, and vents | 20 [kg]                    |
| Heat capacity of the clothes dryer frame  | 0.49 [kJ/kg-K]             |
| Initial mass of water content within cloth  | 5.18 [kg]                  |
| Water heat capacity   | 4.2 [kJ/kg-K]              |
| Desorber temperature  | 110 [°C]                   |
| Air volumetric flow rate  | 305.8 [m <sup>3</sup> /hr] |
| Mass flow rate of the desiccant solution  | 0.02 [kg/s]                |
| Effectiveness of the solution heat exchanger  | 80%                        |
| UA value of the desorber module   | 200 [W/K]                  |
| UA value of the absorber module   | 36 [W/K]                   |
| UA value of the condenser module  | 59 [W/K]                   |
| UA value of the air-to-solution heat exchanger (AS-HX)  | 26 [W/K]                   |
| Initial temperature of the ambient air and cloth  | 25 [°C]                    |
| Initial relative humidity of the air within the drum  | 50%                        |

where  $C_{cl}$  is the closed-loop correction coefficient modifying the open-loop test data presented by Patel et al. [4]. The CEF is calculated as follows:

$$CEF = \frac{m_{clothes}}{(1.5\dot{Q}_{des} + \dot{W}_{blower} + \dot{W}_{drum})Drying\ time} \left[ \frac{lbm}{kWh} \right] \quad (31)$$

The SMER, another efficiency metric, is defined as follows:

$$SMER = \frac{m_{water}}{(1.5\dot{Q}_{des} + \dot{W}_{blower} + \dot{W}_{drum})Drying\ time} \left[ \frac{kg_{water}}{kWh} \right] \quad (32)$$

As evident, in the CEF and SMER calculations, it is assumed that only 67% (i.e., 1/1.5) of the energy generated during the fuel combustion process is transferred to the desorber module.

### 3.4. Modeling algorithm

A modeling algorithm was developed to combine the sorption and dehydration sub-models. The modeling algorithm flowchart is shown in Fig. 3. The algorithm solves the above ordinary differential equations employing a time-marching scheme. The main input parameters to the algorithm include initial material temperature ( $T_{surf,init}$ ), initial air temperature and relative humidity ( $T_{air,init}, \phi_{air,init}$ ), air stream mass flow rate ( $\dot{m}_{air}$ ), solution mass flow rate ( $\dot{m}$ ), water vapor dehumidification rate in the absorber ( $J$ ), overall heat transfer coefficient value for different modules ( $UA$ ), dryer efficiency ( $\epsilon_{dryer}$ ) as a function of RMC, and heat exchanger efficiencies ( $\epsilon$ ). The main outcomes of the algorithm include transient temperature, concentration, humidity variations, and overall SMER, CEF, and drying time.

## 4. Results

A sample clothes dryer with a known experimentally measured heat and mass transfer effectiveness as described in Gluesenkamp et al. [39] was selected to evaluate the performance of the proposed sorption-based gas dehydration concept. As shown in Fig. 4, the heat and mass transfer processes associated with the drum unit are highly effective during most of the drying process. However, the effectiveness starts declining at the later drying stages at which the RMC is about 15%. Considering the U.S. DOE standard test procedure, the mass of bone-dry cloth is assumed 3.83 kg (i.e., 8.45 lbm). Table 1 lists all nominal and constant input parameters to the thermodynamic model.

### 4.1. Transient response of the system at a fixed air flow rate

Fig. 5a shows transient temperature variations of the condenser air outlet (i.e., the drum air inlet), the dehumidifier air outlet, the drum air outlet, and the clothes during the drying process at which the initial RMC drops from 57.5% to 4%. The temperature of the clothes was assumed to be equal to that of the frame. The corresponding variations in relative humidity of the condenser air outlet, the dehumidifier air outlet, and the drum air outlet are shown in Fig. 5b. The results are presented for a fixed air volumetric flow rate of 305.8 m<sup>3</sup>/hr (180 cfm). The air initially enters the dehumidifier module at 25 °C and leaves the condenser module of the desiccant cycle at 58 °C. The rise in the air

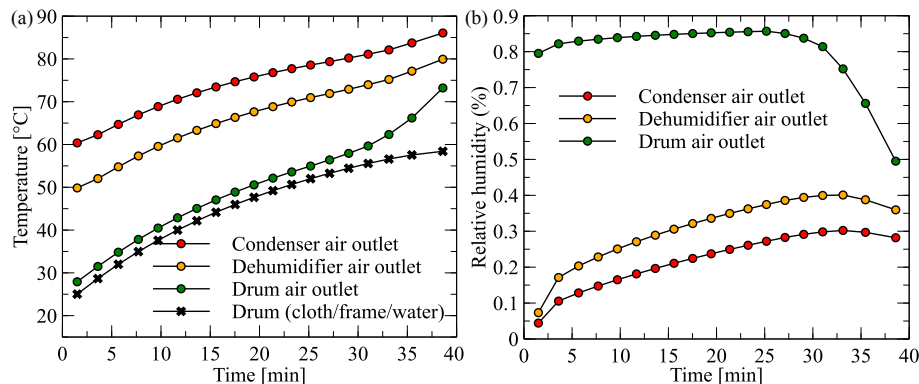


Fig. 5. (a) Transient temperature variations of the condenser air outlet, dehumidifier air outlet, drum air outlet, and drum, and (b) transient variations in relative humidity of the condenser, dehumidifier and drum air outlet.

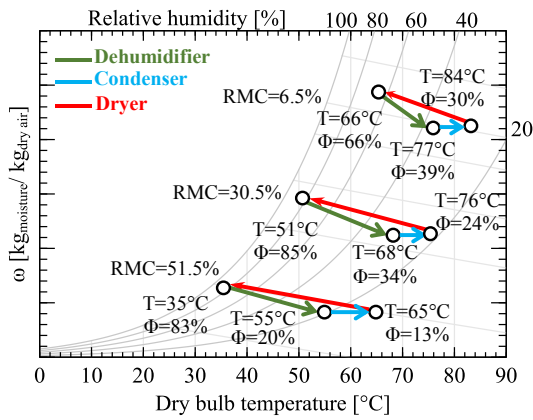


Fig. 6. Psychrometric air flow processes associated with RMC of 51.5% (an early drying stage), 30.5% (an intermediate drying stage), and 6.5% (a late drying stage).

temperature occurs in both dehumidifier and condenser modules of the desiccant cycle. In the drum unit, the drying process reduces the temperature of the air before entering the desiccant cycle to complete the air loop. Simultaneously, the desiccant cycle efficiently dehumidifies the highly humid air leaving the drum unit. As shown in Fig. 5b, the sorption cycle delivers relatively dry air to the drum unit throughout the entire dehydration process such that the maximum relative humidity supplied to the drum unit does not exceed 30%. It can be also understood that the temperatures of clothes and frame body gradually increase from the initial temperature of 25–59 °C as they are heated through sensible heat

exchanged with the air flow stream. Additionally, the temperature of the air leaving the condenser module (i.e., supplied to the drum unit) gradually increases from an initial temperature of 58 °C to a final temperature of 86 °C.

As shown in Fig. 5b, the relative humidity of the air leaving the condenser module of the desiccant cycle slightly increases during the drying process. This is attributed to a rise in the air temperature entering the dehumidifier module, which increases the temperature of the desiccant liquid as the drying process proceeds. A rise in the desiccant temperature can negatively affect the performance of the dehumidifier module leading to a lower moisture removal rate and thus a higher air relative humidity. Furthermore, as shown in Fig. 5a and b, the temperature (relative humidity) of the air leaving the drum unit is substantially lower (higher) than that of the air entering the drum unit. This indicates a high heat and mass transfer effectiveness of the drum unit during most of the drying process as emphasized in Fig. 4. The difference between the temperature and relative humidity of the dryer air inlet and outlet conditions, however, decreases at the later stages of the drying process. This is because the heat and mass transfer effectiveness of the drum unit abruptly declines when the RMC of the clothes is minimal.

To better understand the transient response of the proposed system, time evolutions of the air flow processes involved are drawn in a psychrometric chart. Three representative moments during the drying process are shown in Fig. 6: at high RMC (51.5%), medium RMC (30.5%), and low RMC (6.5%). Each thermodynamic cycle shows the heat and mass transfer processes of the air as it passes through the dehumidifier (green line), condenser (blue line), and drum (red line). The respective thermodynamic conditions of the air and desiccant loops are also presented in Fig. 7. As shown, the average operating temperature of the heat and mass transfer processes involved shifts to higher

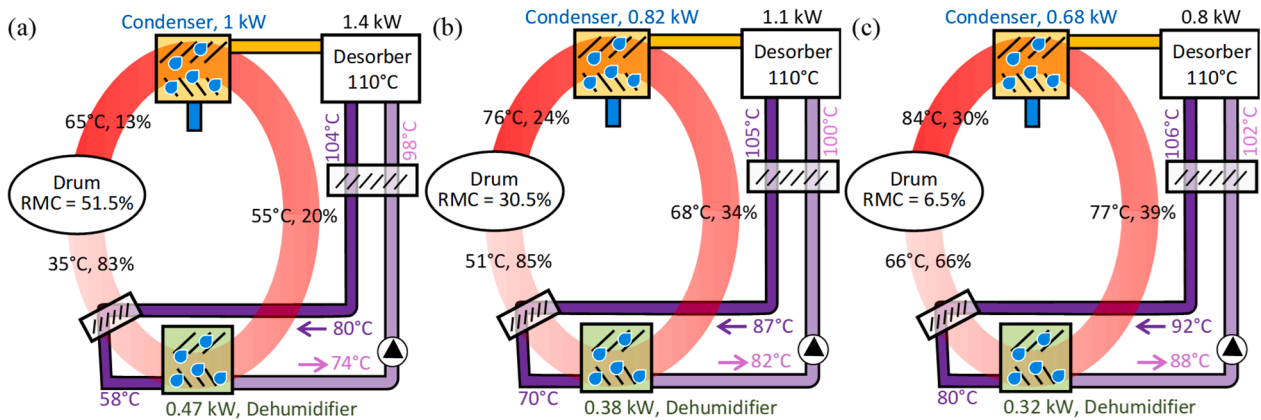


Fig. 7. Thermodynamic conditions of the air and desiccant cycles associated with RMCs of (a) 51.5% (an early drying stage), (b) 30.5% (an intermediate drying stage), and (c) 6.5% (a late drying stage).

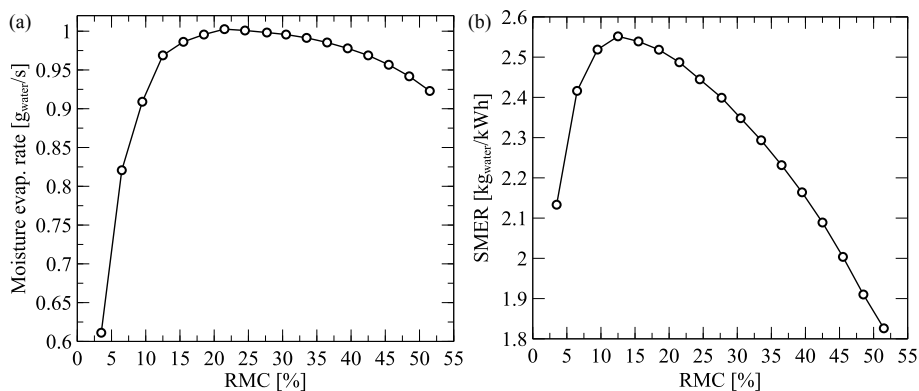


Fig. 8. (a) Transient moisture evaporation rate, and (b) transient CEF/SMER variations as a function of RMC.

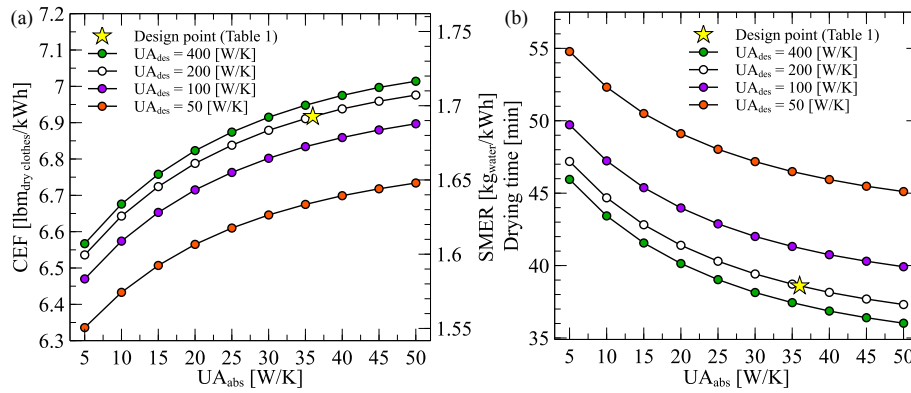


Fig. 9. Variations of (a) the CEF and SMER, and (b) the total drying time versus absorber UA values at different UA values of the desorber module.

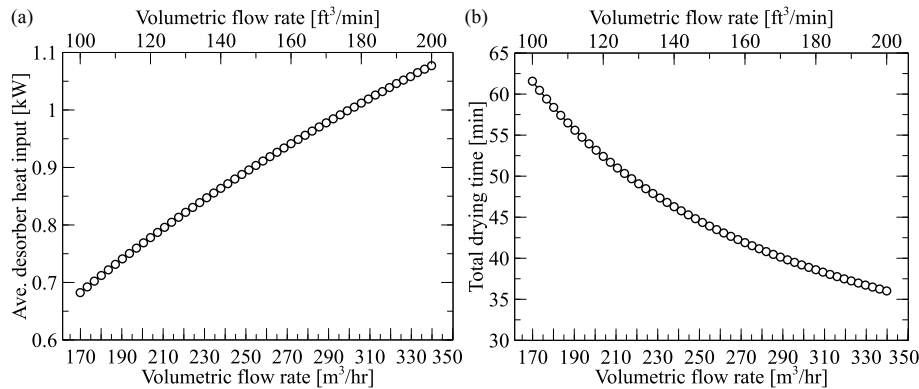


Fig. 10. Effect of air volumetric flow rate on (a) the average desorber heat input, and (b) the total drying time.

values as the RMC decreases. This is mainly attributed to the temperature of the clothes and frame body, which increases as the dehydration process continues. Additionally, the heat input to the desorber module declines as the drying process proceeds. This is because the sensible heat associated with the clothes/water/frame body decreases as they are heated. Furthermore, the total dehumidification rate decreases at higher absorber operating temperatures, which reduces the total thermal energy required for the desorber module.

Fig. 8a and b present transient moisture evaporation rate and SMER as a function of the RMC. The evaporation rate and SMER increase during the early stages of the dehydration process. The thermal energy associated with the air stream entering the drum unit can be divided into the sensible load (i.e., temperature rise in clothes, water, and frame) and

the latent load (i.e., water evaporation process). As the dehydration process proceeds, the temperatures approach a plateau, thereby reducing the contribution of the sensible load. As a result, a larger fraction of the incoming thermal energy is utilized for the latent load, thereby increasing the moisture evaporation rate and SMER at the early stages of the drying process. At low RMC levels, however, the effectiveness of the heat and mass transfer processes involved abruptly drop. This drop significantly deteriorates drying performance and thus reduces the moisture evaporation rate and SMER at later stages of the drying process.

Fig. 9 shows variations of the CEF, SMER, and total drying time versus absorber UA values at different UA values of the desorber module. The drying performance metrics associated with the design point (i.e., Table 1) are labeled with a star. At a fixed desorber UA value, the proposed sorption-based gas clothes dryer system becomes more efficient and offers a shorter drying time when the UA value of the absorber module increases. This is attributed to the dehumidification capacity of the proposed system, which increases at higher absorber UA values. This subsequently improves the drying performance metrics of the system. The CEF, SMER, and total drying time, however, approach a plateau at high absorber UA values. Similarly, at a fixed absorber UA value, the proposed drying system demonstrates higher CEFs and faster drying rates when the desorber UA value increases. This is because the water vapor desorption rate and subsequent condensation rate are improved as the desorber UA value increases. This, in turn, augments the CEF and shortens the drying time of the proposed system. The sensitivity of the drying performance metrics to the desorber module, however, diminishes at high desorber UA values.

#### 4.2. Overall response of the system at different air flow rates

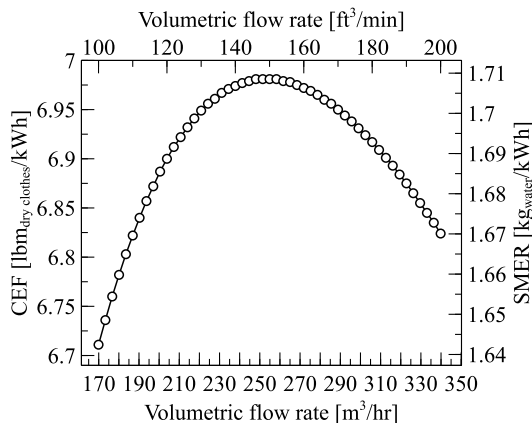


Fig. 11. Average CEF and SMER as a function of the air volumetric flow rate.

Fig. 10a and b show the effect of air volumetric flow rate on the

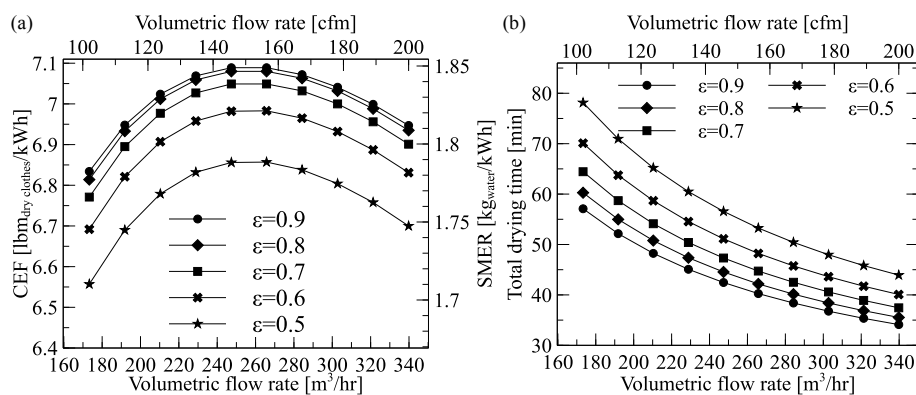


Fig. 12. Variations of (a) the CEF and SMER, and (b) the total drying time versus air volumetric flow rate at different dryer effectivenesses.

average desorber heat input and total drying time. As evident, the air flow rate strongly affects important drying performance metrics. As the air volumetric flow rate increases, the thermal energy carried by the circulating air stream boosts, thereby increasing the moisture quantity vaporized. Subsequently, the heat input to the desorber module increases to reject the additional laundry moisture captured (cf. Fig. 10a). The results indicate that the desorber heat input increases by 61% (from 0.67 to 1.08 kW) when the air volumetric flow rate increases by 100% (i.e., from 169.9 to 339.8 m<sup>3</sup>/hr). Additionally, the moisture content removed increases at higher air flow rates, thereby decreasing the total drying time (cf. Fig. 10b). For instance, the total drying time decreases from 63 to 36 min, a 43% improvement in the total drying time, when the air volumetric flow rate increases by 100% (i.e., from 169.9 to 339.8 m<sup>3</sup>/hr).

Fig. 11 shows the average CEF and SMER as a function of the air volumetric flow rate. The CEF and SMER values represent the drying energy efficiency considering the effects of both desorber heat input (cf. Fig. 10a) and drying time (cf. Fig. 10b). At low air volumetric flow rates close to 169.9 m<sup>3</sup>/hr (100 cfm), the CEF and SMER performance metrics are low due to a long drying time, meaning that lower energy consumption became significant. At high air volumetric flow rates close to 339.8 m<sup>3</sup>/hr (200 cfm), the CEF and SMER rates are moderate owing to a high desorber heat input and a high air blower power required. The CEF and SMER rates are maximized at an intermediate air volumetric flow rate of 254.9 m<sup>3</sup>/hr (150 cfm), where the desorber heat input and total drying time are medium. The thermodynamic analysis indicates the proposed sorption-based gas clothes dryer system can deliver a SMER of 1.71 kg<sub>water</sub>/kWh and a CEF of 3.167 kg (6.98 lbm) of dry cloth per kWh with a drying time of 44 min at an air volumetric flow rate of 254.9 m<sup>3</sup>/hr (150 cfm). This is a 112% energy improvement compared with state-of-the-art gas clothes dryers exhibiting a CEF of 1.50 kg (3.3 lbm) of dry cloth per kWh [37].

#### 4.3. Implications for other dehydration processes with varying drum effectiveness

The above results clearly demonstrate the advantages of the proposed sorption-based gas clothes dryer concept with a known drum effectiveness profile over conventional dryers. Dehydration systems employed in other industrial sectors may present different heat and mass transfer effectiveness depending on their products' shape factor, air flow distribution, surface area, and dryer architecture. Therefore, examining the effect of drum effectiveness on the overall performance metrics of the system is useful. Fig. 12 shows variations of the CEF, SMER, and total drying time versus air flow rates at different drum effectivenesses. At a fixed drum effectiveness, the overall trends of CEF, SMER, and total drying time curves are similar to those of a variable drum effectiveness as studied earlier (cf. Figs. 10b and 11). In other words, the CEF and SMER peak at an intermediate air flow rate and the drying time

decreases with the air flow rate. Additionally, it is evident that the drying performance metrics are improved (i.e., higher CEF and SMER at shorter dryer times) when the drum effectiveness increases. Although the improvement in the energy performance is marginal (i.e., from 3.11 kg to 3.22 kg of dry cloth per kWh or a 3.5% difference), the drying time meaningfully decreases from 57 to 43 min (i.e., a 25% difference) when the drying effectiveness increased from 0.5 to 0.9 at a fixed air volumetric flow rate of 254.9 m<sup>3</sup>/hr (150 cfm).

## 5. Conclusions

This study introduced an innovative sorption-based dehydration concept to overcome barriers deteriorating energy efficiency in existing gas, electric, or heat pump dryer systems. A detailed quasi-steady-state thermodynamic model was developed to evaluate the dehydration performance of the new concept employed for a gas clothes dryer application. The transient temperature, relative humidity, moisture evaporation rate, and CEF variations provided thorough information on the system's transient response during the drying process. Particularly, it was found that the instantaneous moisture removal rate and CEF/SMER are maximized at an intermediate RMC level.

The thermodynamic model predicted that a more energy-efficient but slower drying process can be realized at a low air volumetric flow rate close to 169.9 m<sup>3</sup>/hr (100 cfm). Conversely, a less energy-efficient but faster drying process is achievable at a high air volumetric flow rate close to 339.8 m<sup>3</sup>/hr (200 cfm). Furthermore, the results indicated the overall SMER and CEF of the proposed sorption-based gas clothes dryer system are maximized at an intermediate air volumetric flow rate of 254.9 m<sup>3</sup>/hr (150 cfm). At this state, the overall SMER is 1.71 kg<sub>water</sub>/kWh (i.e., CEF of 6.98 lbm<sub>dry clothes</sub>/kWh) with a drying time of 44 min, reflecting a 112% energy improvement compared with state-of-the-art gas clothes dryers. The promising drying performance metrics shown here demonstrate the potential of the proposed sorption-based gas dehydration system for other fuel-driven equipment to take advantage of available waste thermal energy in the environment and improve energy efficiency.

#### CRediT authorship contribution statement

**Masoud Ahmadi:** Investigation, Data curation, Visualization, Writing - original draft. **Kyle R. Gluesenkamp:** Writing - review & editing. **Sajjad Bigham:** Conceptualization, Supervision, Methodology, Visualization, Writing - original draft, Writing - review & editing.

#### Declaration of Competing Interest

The authors declare that they have no known competing financial interests or personal relationships that could have appeared to influence the work reported in this paper.

## Acknowledgments

This study was sponsored by the US Department of Energy's Office of Energy Efficiency and Renewable Energy (EERE) under the Building Technology Office Award Number DEEE0008685. The authors would like to acknowledge Mr. Antonio Bouza, Technology Manager, Mr. Mohammed Khan, Technical Project Officer, and Mr. Michael Geocaris, Project Engineer, HVAC, Water Heating, and Appliance subprogram, Building Technologies Office, US Department of Energy. The authors also acknowledge Olivia Shafer for proofreading.

## References

- [1] Dai B, Zhao P, Liu S, Su M, Zhong D, Qian J, et al. Assessment of heat pump with carbon dioxide/low-global warming potential working fluid mixture for drying process: energy and emissions saving potential. *Energy Convers Manage* 2020;222: 113225. <https://doi.org/10.1016/j.enconman.2020.113225>.
- [2] El Hage H, Herez A, Ramadan M, Bazzi H, Khaled M. An investigation on solar drying: a review with economic and environmental assessment. *Energy* 2018;157: 815–29. <https://doi.org/10.1016/j.energy.2018.05.197>.
- [3] U.S. Energy Information Administration, Annual Energy Outlook 2017. 2017.
- [4] Patel VK, Gluesenkamp KR, Goodman D, Gehl A. Experimental evaluation and thermodynamic system modeling of thermoelectric heat pump clothes dryer. *Appl Energy* 2018;217:221–32. <https://doi.org/10.1016/j.apenergy.2018.02.055>.
- [5] Bansal P, Sharma K, Islam S. Thermal analysis of a new concept in a household clothes tumbler dryer. *Appl Energy* 2010;87:1562–71. <https://doi.org/10.1016/j.apenergy.2009.10.029>.
- [6] TeGrotenhuis W, Butterfield A, Caldwell D, Crook A, Winkelman A. Modeling and design of a high efficiency hybrid heat pump clothes dryer. *Appl Therm Eng* 2017; 124:170–7. <https://doi.org/10.1016/j.applthermaleng.2017.05.048>.
- [7] Ng AB, Deng S. A new termination control method for a clothes drying process in a clothes dryer. *Appl Energy* 2008;85:818–29. <https://doi.org/10.1016/j.apenergy.2007.10.016>.
- [8] Stawreberg L, Nilsson L. Potential energy savings made by using a specific control strategy when tumble drying small loads. *Appl Energy* 2013;102:484–91. <https://doi.org/10.1016/j.apenergy.2012.07.045>.
- [9] Bansal PK, Braun JE, Groll EA. Improving the energy efficiency of conventional tumble clothes drying systems. *Int J Energy Res* 2001;25:1315–32. <https://doi.org/10.1002/er.752>.
- [10] Jian Q, Luo L. The improvement on efficiency and drying performance of a domestic venting tumble clothes dryer by using a heat pipe heat recovery heat exchanger. *Appl Therm Eng* 2018;136:560–7. <https://doi.org/10.1016/j.applthermaleng.2018.03.029>.
- [11] Cochran M, Goodnight J, Babin B, Eckels S. Condensing dryers with enhanced dehumidification using surface tension elements. *Appl Therm Eng* 2009;29: 723–31. <https://doi.org/10.1016/j.applthermaleng.2008.03.050>.
- [12] Jian Q, Zhao J. Drying performance analysis of a condensing tumble clothes dryer with a unique water cooled heat exchanger. *Appl Therm Eng* 2017;113:601–8. <https://doi.org/10.1016/j.applthermaleng.2016.11.086>.
- [13] Martin E, Sutherland K, Parker D. Measured performance of heat pump clothes dryers (FSEC-RR-645-16). ACEEE Summer Study Energy Effic Build 2016;2016: 1–13.
- [14] Do Y, Kim M, Kim T, Jeong S, Park S, Woo S, et al. An experimental study on the performance of a condensing tumble dryer with an air-to-air heat exchanger. *Korean J Chem Eng* 2013;30:1195–200. <https://doi.org/10.1007/s11814-013-0037-4>.
- [15] Stawreberg L, Nilsson L. Modelling of specific moisture extraction rate and leakage ratio in a condensing tumble dryer. *Appl Therm Eng* 2010;30:2173–9. <https://doi.org/10.1016/j.applthermaleng.2010.05.030>.
- [16] Yadav V, Moon CG. Fabric-drying process in domestic dryers. *Appl Energy* 2008; 85:143–58. <https://doi.org/10.1016/j.apenergy.2007.06.007>.
- [17] Ameen A, Bari S. Investigation into the effectiveness of heat pump assisted clothes dryer for humid tropics. *Energy Convers Manage* 2004;45:1397–405. <https://doi.org/10.1016/j.enconman.2003.09.001>.
- [18] Krokida MK, Bisharat GI. Heat recovery from dryer exhaust air. *Drying Technol* 2004;22:1661–74. <https://doi.org/10.1081/DRT-200025626>.
- [19] Cao T, Ling J, Hwang Y, Radermacher R. Development of a novel two-stage heat pump clothes dryer. ASME Int. Mech. Eng. Congr. Expo. Proc., vol. 6A, American Society of Mechanical Engineers (ASME); 2014. <https://doi.org/10.1115/IMECE2014-36048>.
- [20] Goh LJ, Othman MY, Mat S, Ruslan H, Sopian K. Review of heat pump systems for drying application. *Renew Sustain Energy Rev* 2011;15:4788–96. <https://doi.org/10.1016/j.rser.2011.07.072>.
- [21] Pierucci S, Klemes JJ, Piazza L, Bakalis S, Walmsley TG, Klemes JJ, et al. Innovative hybrid heat pump for dryer process integration. *Chem Eng Trans* 57: 2017.
- [22] T'Jollyn I, Lecompte S, Vanslambrouck B, De Paep M. Energetic and financial assessment of the implementation of an absorption heat pump in an industrial drying system. *Drying Technol* 2019;37:1939–53. <https://doi.org/10.1080/07373937.2018.1546190>.
- [23] Jollyn IT, Paep M De. Thermal analysis of absorption heat pump implementation in an industrial dryer. 12th Int. Conf. Heat Transf. Fluid Mech. Thermodyn. Costa del Sol, Spain, July 2016; 2016.
- [24] Gabas AL, Bernardi M, Telis-romero J, Telis VRN. Application of heat pump in drying of apple cylinders. Proc. 14th Int. Dry. Symp. (IDS 2004) São Paulo, Brazil, 22–25 August 2004; 2004.
- [25] Le Lostec B, Galanis N, Baribeault J, Millette J. Wood chip drying with an absorption heat pump. *Energy* 2008;33:500–12. <https://doi.org/10.1016/j.energy.2007.10.013>.
- [26] Jangam SV, Joshi VS, Mujumdar AS, Thorat BN. Studies on dehydration of Sapota (Achras zapota). *Drying Technol* 2008;26:369–77. <https://doi.org/10.1080/07373930801898190>.
- [27] Sagar VR, Suresh Kumar P. Recent advances in drying and dehydration of fruits and vegetables: a review. *J Food Sci Technol* 2010;47:15–26. <https://doi.org/10.1007/s13197-010-0010-8>.
- [28] Aktaş M, Taşeri L, Şevik S, Gülcü M, Uysal Seçkin G, Dolgun EC. Heat pump drying of grape pomace: performance and product quality analysis. *Drying Technol* 2019; 37:1766–79. <https://doi.org/10.1080/07373937.2018.1536983>.
- [29] Liu M, Wang S, Liu R, Yan J. Energy, exergy and economic analyses on heat pump drying of lignite. *Drying Technol* 2019;37:1688–703. <https://doi.org/10.1080/07373937.2018.1531883>.
- [30] Minea V. Efficient energy recovery with wood drying heat pumps. *Drying Technol* 2012;30:1630–43. <https://doi.org/10.1080/07373937.2012.701261>.
- [31] Jangam S V., Mujumdar AS. Heat pump assisted drying technology – overview with focus on energy, environment and product quality. Mod. Dry. Technol., vol. 4, Wiley-VCH; 2012. p. 121–62. <https://doi.org/10.1002/9783527631681.ch4>.
- [32] Liu Di, Zhao F-Y, Tang G-F. Modeling and performance investigation of a closed-type thermoelectric clothes dryer. *Drying Technol* 2008;26:1208–16. <https://doi.org/10.1080/07373930802306995>.
- [33] Bigham S, Yu D, Chugh D, Moghaddam S. Moving beyond the limits of mass transport in liquid absorbent microfilms through the implementation of surface-induced vortices. *Energy* 2014;65:621–30. <https://doi.org/10.1016/j.energy.2013.11.068>.
- [34] Bigham S, Nasr Isfahani R, Moghaddam S. Direct molecular diffusion and micro-mixing for rapid dewatering of LiBr solution. *Appl Therm Eng* 2014;64:371–5. <https://doi.org/10.1016/j.applthermaleng.2013.12.031>.
- [35] Moghaddam S, Bigham S, Chugh D, Nasr Isfahani R, Fazeli A, Yu D, et al. Open absorption cycle for combined dehumidification, water heating, and evaporating cooling; 2017. <https://doi.org/https://patents.google.com/patent/WO2015116362A1/en>.
- [36] Herold K, Radermacher R, Klein S. Absorption chillers and heat pumps. 2nd ed. Taylor & Francis Group; 2016. <https://doi.org/10.1201/b19625>.
- [37] U.S. DOE federal standards, 10 CFR 430.32 (h), Energy and Water Conservation Standards and Compliance Dates; 2013.
- [38] Shen B, Gluesenkamp K, Beers D. Heat pump clothes dryer model development. Int. Refrig. Air Cond. Conf. Purdue Univ. West Lafayette, Indiana, July 11–14, 2016; 2016, p. Paper 1755.
- [39] Gluesenkamp KR, Boudreaux P, Patel VK, Goodman D, Shen Bo. An efficient correlation for heat and mass transfer effectiveness in tumble-type clothes dryer drums. *Energy* 2019;172:1225–42. <https://doi.org/10.1016/j.energy.2019.01.146>.